

Distribution of Internal Stresses across Automotive Windshields: A First Step to Characterize the Post-fracture Behaviour

Nils Meinhard ^a, Bekir Kacmaz ^b, Miriam Schuster ^a, Christian Alter ^b, Stefan Kolling ^b, Michael Kraus ^a

- a. Glass Competence Center, Institute of Structural Mechanics and Design, TU Darmstadt, Germany
- b. Institute for Mechanics and Materials, THM University of Applied Sciences, Wiesenstraße 14, Gießen, 35394, Germany

Abstract

For pedestrian safety in car crashes, estimating the Head Injury Criterion (HIC) in head impact tests on windshields has significant importance. This requires evaluating the acceleration profile experienced by the head impactor over the entire crash duration. In a previous project, a stochastic failure model was developed to accurately simulate the behaviour of windshields up to the point of glass fracture. Automotive windshields are typically made of laminated safety glass (LSG), consisting of two glass layers bonded by a polymeric interlayer made of polyvinyl butyral (PVB). This laminate retains glass fragments post-breakage and provides a residual load bearing capacity. However, characterizing this post-fracture behaviour has not yet been adequately achieved.

A recent research project aims to develop an approach that accounts for the post-fracture behaviour of LSG in numerical simulation. For this purpose, the residual stiffness and load bearing capacity of fractured LSG will be measured on small samples under different strain rates and fragmentation grades. These results will then be incorporated into a numerical model, which will be validated through tests on full-scale windshields. A methodology will be established to predict the fracture pattern across the windshield, which depends on the elastic strain energy in the glass panes. As a first result of the research project, the paper presents the distribution of internal stresses across the windshield. These stresses arise from the production process, particularly the shaping process of the curved windshield, and play a crucial role in determining the fracture pattern. By analysing these internal stresses, the study focusses on insights into the mechanisms influencing glass failure, which is largely governed by the dissipation energy released upon impact.

Keywords

Glass strength, Laminated safety glass, Automotive windscreen, Curved glass, Post-fracture behaviour, Fracture pattern

Article Information

- Published by [Glass Performance Days](#), on behalf of the author(s)
- Published as part of the Glass Performance Days Conference Proceedings, June 2025
- Editors: Jan Belis, Christian Louter & Marko Mökkönen
- This work is licensed under a [Creative Commons Attribution 4.0 International](#) (CC BY 4.0) license.
- Copyright © 2025 with the author(s)

1. Introduction

According to the World Health Organization (WHO), the number of traffic fatalities worldwide is approximately 1.35 million people annually (World Health Organization, 2018). This makes road traffic accidents the eighth leading cause of death globally. A particular risk for vulnerable road users is head impact with the vehicle's hood. To assess the potential severity of injuries occurring in such cases, head impactors are shot onto the relevant areas of a car in laboratory settings. Such a head impact test on a windshield can be seen in Fig. 1. The translational accelerations of the impactor are measured, and from the resultant acceleration a_{res} , the Head Injury Criterion (HIC (eq. 1)) is derived.

$$HIC = \left[\frac{1}{t_2 - t_1} \int_{t_1}^{t_2} a_{res}(t) dt \right]^{2.5} (t_2 - t_1) \quad (1)$$

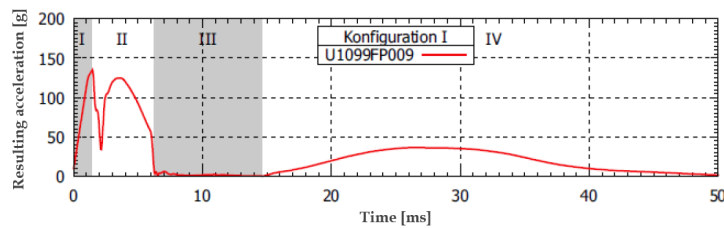
The time limits t_1 and t_2 are adjusted in such a way that the resulting HIC is maximized, in order to account for the worst-case scenario.



Fig. 1: Full size impact test on windshield.

Windshields are made of laminated glass, typically consisting of two glass panes bonded together by a PVB-based interlayer. After breaking, the fragments remain attached to the polymer interlayer, allowing the laminate to retain a residual load-bearing capacity that prevents the impactor from passing through the glass. The glass is neither thermally nor chemically pre-stressed, as pre-stressed glass would break suddenly over the entire surface upon crack formation. This type of breakage is undesirable in windshields because, in the event of failure, it would severely impair visibility and potentially lead to the complete failure of the windshield due to a single impact, such as a stone strike. However, residual stresses can still be measured within the glass. Previous studies (BMW-Projekt 18295N, 2020) suggest that these stresses result from the manufacturing process. This includes heating up the windscreen to 600°C, bending, and then cooling the glass in an industrial process.

The determination of the HIC value for the windshield and the corresponding description of the post-fracture behavior is usually carried out through destructive tests on full scale windshields, which are costly and time-consuming. This creates the demand to replace these tests with numerical simulations. An example of the impactor's resultant acceleration curve during an impact test is shown in Fig. 2. In the initial part of the curve, the first contact of the impactor with the windscreen is seen, causing the first layer of the laminate to break, followed by the second layer. The sudden release of energy upon breakage often results in the breaking glass moving away from the impactor, after which the impactor enters a free-flight phase. The impactor then hits the now-broken glass again and remains on the laminate.



Section I:	Both panes are intact
Section II:	Sudden change in stiffness due to the fracture of the first and second pane
Section III:	Free-flight phase
Section IV:	Post-breakage behaviour

Fig. 2: Impactor's acceleration curve during an impact test from (Alter, 2019).

The first three stages of the curve, up to the post-breakage behaviour, can be sufficiently described numerically by a stochastic model (BMW-Projekt 18295N, 2020; BMBF-Projekt 17N1111, 2014). However, post-breakage behaviour can only be qualitatively described so far. Since the final section of the curve can have significant influence on the HIC assessment, it must be thoroughly investigated. Many influencing parameters play a role here. These include, for example, the load and support boundary conditions, the degree of glass fragmentation, the mechanical properties of the interlayer – which depend on component temperature, humidity, and load duration – and the adhesion between the glass and the interlayer. The influence of the fracture pattern on post-fracture behaviour has been investigated, for example, in (Boilzi, Orlando, Piscitelli, & Spinelli, 2016; Hooper, 2011; Angelides, Talbot, & Overend, 2021; Anglides, 2022; Zhao, Yang, Wang, & Azim, 2019), the influence of different strain rates in (Boilzi, Orlando, Piscitelli, & Spinelli, 2016; Botz, 2020; Hooper, 2011; Seshadri, Bennison, Jagota, & Saigal, 2002), the influence of different temperatures in (Wellershoff & Illguth, 2021; Angelides, Talbot, & Overend, 2021; Anglides, 2022; Samieian, et al., 2018), and the influence of adhesion levels in (Wellershoff & Illguth, 2021; Seshadri, Bennison, Jagota, & Saigal, 2002). In summary, it was observed – regardless of specimen type and test setup – that the adhesion of fracture fragments to the interlayer leads to a stiffening effect compared to the behaviour of the interlayer material alone. Additionally, it was found that the initial stiffness decreases with an increasing degree of fragmentation and in the presence of concentric cracks in both glass layers of the laminate. However, with a higher strain rate or lower temperature, the initial stiffness increases. Furthermore, it was determined that low adhesion leads to high delamination and a reduced stiffness response of the laminate.

A pivotal aspect of understanding post-breakage behaviour lies in accurately predicting the breakage pattern and the local degree of fragmentation of the windshield. This pattern is influenced by both the deformation energy E_u due to elastic deformation at the moment of impact, i.e. through external loading, and the windshield's initial state, characterized by pre-existing residual stresses and the corresponding Energy $E_{residual\ stress}$. Together, these sum up to the total energy E_{total} (eq. 2).

$$E_{total} = E_{residual\ stress} + E_u \quad (2)$$

It is known from the literature (Akeyoshi & Kanai, 1965; Lee, Cho, Yoon, & Lee, 2012; Mognato, Brocca, & Barbieri, 2017; Pourmoghaddam & Schneider, 2019; Nielsen & Bjarrum, 2017; Pourmoghaddam, 2019) that the fracture pattern of tempered glass depends on the glass thickness and the degree of prestressing (or the energy density resulting from the residual stresses). For the same glass thickness, higher residual stresses lead to significantly smaller fracture fragments compared to lower residual stresses. Therefore, exploring and quantifying internal energy development during the impact and pre-existing residual stresses are crucial in enhancing predictive models of post-breakage behaviour. During an impact, the kinetic energy transferred to the windshield can be obtained by monitoring the internal energy values of the model elements during numerical analysis. Since the strain energy at a single integration point provides only localized information, and the degree of fragmentation relates to

a currently unknown spatial distribution, the energies in the simulation are evaluated over a comparable averaging domain. Figure 3 displays the averaged strain energy in a quasi-static head impact test at a specific moment just before fracture occurs in experimental studies. The graphs in the left column of the figure represent fixed square regions with an edge length of 100mm, while the right column shows continuous averaging using a circular domain with a radius of 50mm. A high energy level does not necessarily equate to a high fragmentation rate, here. Instead, a high energy level indicates that if a crack runs through a high-energy region, a high fragmentation rate will likely occur there. As described, there are also residual stresses and their corresponding Energy present in the windshield, influencing the crack pattern. These can be determined experimentally, which will be focus of this paper.

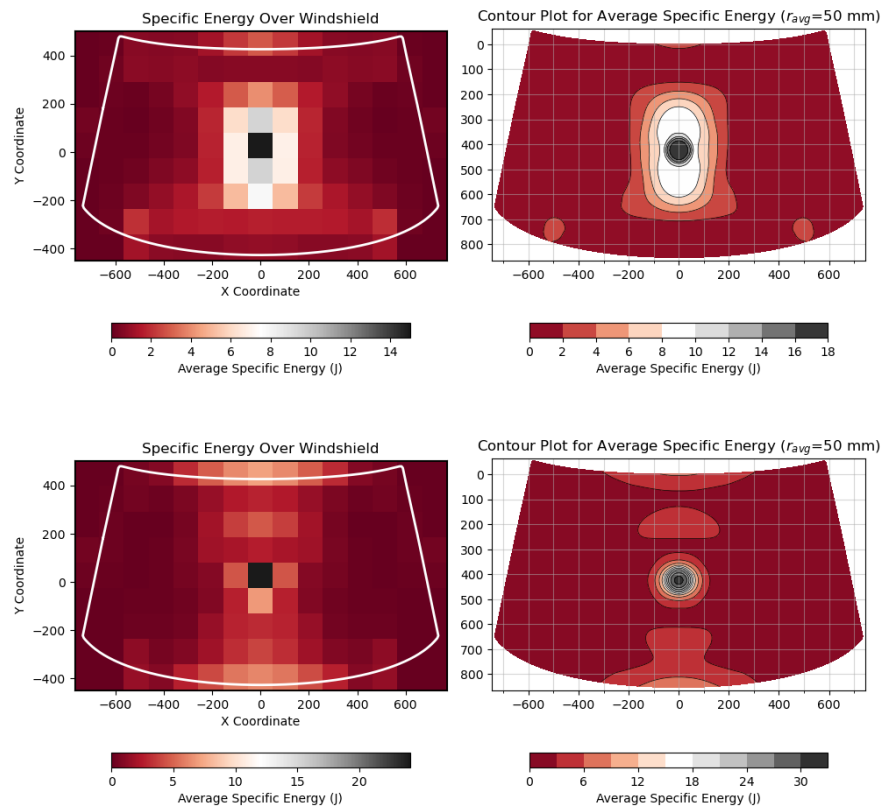


Fig. 3: Specific energy grids and averages for upper and bottom glass panes upon impact.

2. Methods

The residual stresses in the windshield are quantitatively measured using Scattered Light Polarimeters (SCALP) through the glass thickness. The "scattered light method" involves directing a laser through a prism at an angle into the glass. To avoid refraction at the glass-prism interface, an immersion liquid with a refractive index similar to that of the glass is used. The incident light is circularly polarized, and the polarization direction is varied during measurement. Cameras are used to capture the intensity of the backscattered light, from which the phase shift through the glass thickness is determined. Using the stress-optical constant (C) of the glass, the principal stresses can be derived with equation (3).

$$\Delta s = C \cdot (\sigma_1 - \sigma_2) \cdot d \quad (3)$$

Thus, three measurements in three directions x , y and p are required at each measurement point, where p is 45° . From these, the principal stresses σ_1 and σ_2 and corresponding principal directions φ_1 and φ_2 can be derived equation (4) – (7) (Gross, Hauger, Schröder, & Wall, 2014).

$$\tau_{xy} = \sigma_p - \frac{\sigma_y - \sigma_x}{2}, \quad (4)$$

$$\varphi_1 = \frac{1}{2} \arctan\left(\frac{2\tau_{xy}}{\sigma_x - \sigma_y}\right), \varphi_2 = \varphi_1 + \frac{\pi}{2}, \quad (5)$$

$$\sigma_1 = \frac{\sigma_x + \sigma_y}{2} + \frac{\sigma_x - \sigma_y}{2} \cos(2\varphi_1) + \tau_{xy} \sin(2\varphi_1), \quad (6)$$

$$\sigma_2 = \frac{\sigma_x + \sigma_y}{2} + \frac{\sigma_x - \sigma_y}{2} \cos(2\varphi_2) + \tau_{xy} \sin(2\varphi_2). \quad (7)$$



Fig. 4: Grid pattern of the windshield (left) and SCALP measurement on a curved pane (right).

Three laminated glass panels with glass thicknesses of 1.8 mm and a PVB-interlayer thickness of 0.76 mm were analysed in a 10 cm x 10 cm grid (see Fig. 4). Since measurements on the windshield proved to be very complex due to the curvature of the glass, only one laminate was measured over the entire surface. The other two laminates were used for verification and were measured with a coarser grid and fewer measurement points. Black printing is applied to the edges of the windshield. On position 4 (compare Fig. 5), the black print is directly applied to the glass, limiting the SCALP measurements. For the other pane, the black print is applied to position 2, facing the interlayer. However, measurements in this area did not yield meaningful results.

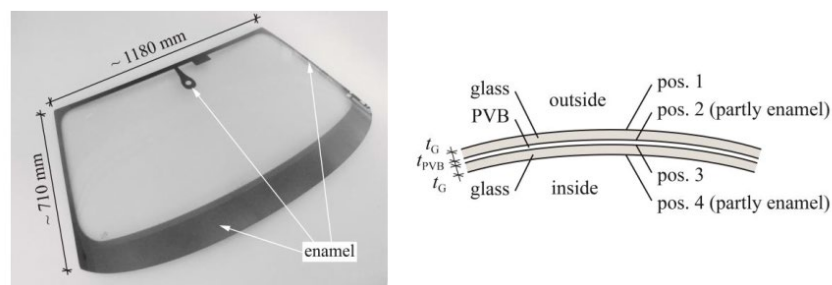


Fig. 5: Dimensions and location of the black print from [2].

Given the scale of the residual stresses in the glass, it is crucial to ensure stress-free support of the laminate. Previous studies (BMW-Projekt 18295N, 2020) attempted to achieve this by placing the glass on an air cushion. After determining that the windshield still leaned on the cushion, it was additionally placed on two identical windshields, thereby reducing the influence of bending due to dead load. In this paper, the experimental set-up was optimized. There are no stresses from bending when the laminate can be laid in accordance with its shape and curvature. To achieve this, frames made of construction foam were sprayed directly onto the windshield to conform to its shape. To increase the rigidity of this construction and compensate for any unevenness in the foam, a wooden frame was attached to the back of the structure (see Fig. 6, left). Lastly, to correct any remaining unevenness from

the foam curing process, a flat air cushion was placed on the frame. For the measurements, the panes were then placed on the air cushion (see Fig. 6, right).



Fig. 6: Support construction made of construction foam (left), setup for SCALP measurements (right).

3. Results

Overall, measurements on the position 4 of the laminated glass were significantly more challenging than those on position 1. Due to the curvature of the glass, a small air gap formed where the SCALP apparatus directed the laser into the glass. While this gap was partially compensated by the immersion liquid, it resulted in non-meaningful measurements at the edges of the glass, as the curvature increases there, as seen in Fig. 8. The measurement area was therefore limited toward the edges. Additionally, at the stress level at which the windshields are, the SCALP is also inherently associated with non-negligible inaccuracies. According to the manual (Glasstress Ltd., Ver. 5.8.5), the precision at stresses <4 MPa is up to 1 MPa. This corresponds to an inaccuracy of up to 25% for measurements in magnitudes that are indeed found in the windshield.

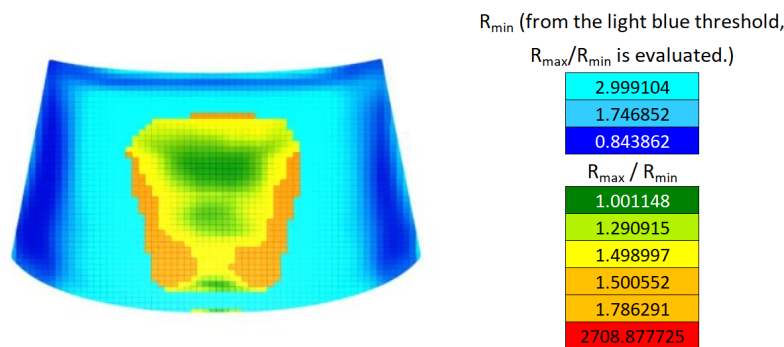


Fig. 7: Curvature radii across the windscreen from (BMW-Projekt 18295N, 2020).

Focusing on the residual stresses on the surface of the windshield, Fig. 7 shows the first and second principal stresses σ_1 and σ_2 and their associated principal directions φ_1 and φ_2 of pos. 1 of the windshield. The stresses are anisotropic across the entire windshield, with the first principal direction aligned vertically across the surface. At the edges, the stresses align toward the edges. At corners, however, the stresses align orthogonal to the corners. The compressive surface stresses range from approximately 8 MPa across the surface, increasing to 16 MPa at the edges. However, in both cases, the overall pattern is not strictly directed toward the corners, suggesting that the bending stresses due to the glass's weight were largely eliminated. In previous studies (BMW-Projekt 18295N, 2020; BMBF-Projekt 17N1111, 2014), even after optimizing the support, the principal stresses were strictly aligned to the corners and had overall a slightly higher stress level. This suggests that there were still bending stresses present there.

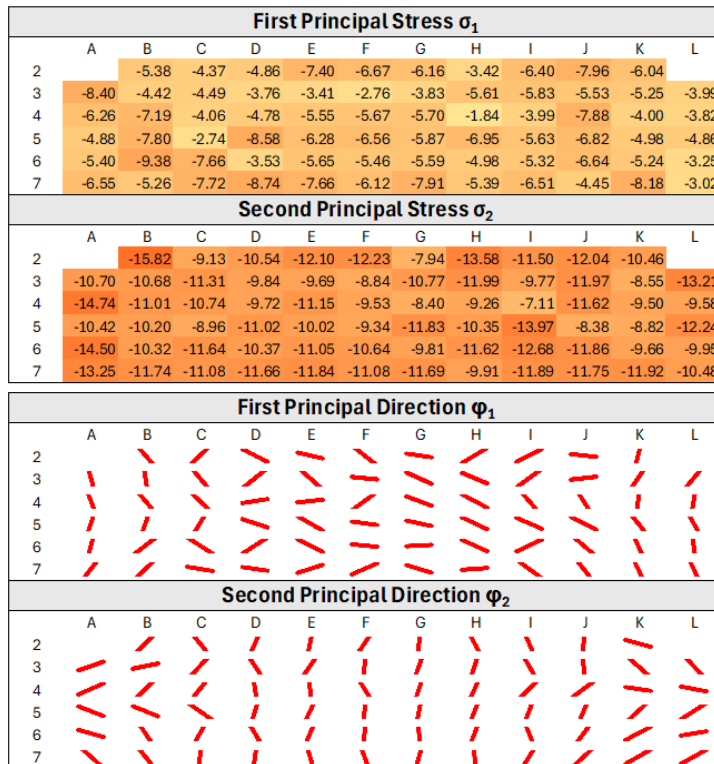


Fig. 8: First and second principal stresses and directions across the windscreen on pos. 1.

Since SCALP measurements, as described, are subject to inaccuracies, and the measurements on the pane yield varying results depending on the curvature radii, the displayed results should be interpreted less as statements about individual measurement points and more as an overall statement about the stress level across the entire pane.

For crash simulations, however, not only the compressive surface stresses of the glass panes (position 1 and 4) are relevant. Rather, the stored energy is determined by the integral of the stresses across the glass thickness. Fig. 9 shows two examples of SCALP measurements on the windshield up to a measurement depth of 1.5 mm. The stress profile is truncated toward the PVB interlayer, where measurements become unreliable. The profile qualitatively resembles that of thermally pre-stressed glass, with compressive stresses on the surfaces and a parabolic shape forming in the tensile zone across the glass thickness. In thermally tempered glass, this distribution is in most cases symmetrical over the glass thickness (Nielsen, Thiele, Schneider, & Meyland, 2021). As shown in Fig. 9, one of the two measurements corresponds very well to this criterion. For thermally tempered glass, this stress profile results from the viscous behaviour of the glass at high temperatures, transitioning to linear elastic behaviour as the glass cools rapidly. Since a similar stress profile is observed in the windshield, it is assumed that the residual stresses in the glass result from the bending process. This is also an explanation for the increasing residual stresses towards the edges. The edges and corners represent geometric thermal bridges, which cool down much faster than the center of the pane during the cooling process. The consequence is higher residual stresses at the edges. Nevertheless, there are also stress distributions observed that were not clearly symmetrically distributed across the pane thickness (compare Fig. 9). These can be explained either by measurement inaccuracies or are induced by an uneven cooling process, investigated by (Nielsen, Thiele, Schneider, & Meyland, 2021).

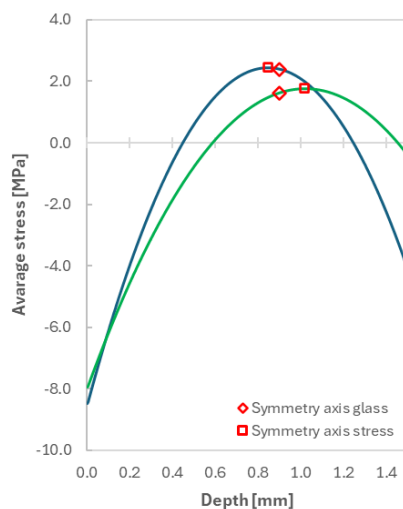


Fig. 9: SCALP measurements distributed over the glass thickness up to a measurement depth of 1.5 mm.

4. Conclusion

This paper presents SCALP measurements in windscreen, which is a first step in describing the post-breakage behaviour during a head impact. The measured surface stresses ranged from 2 to 15 MPa, with an increasing stress level toward the edges. By integrating the shown stresses, the energy level that significantly influences the fracture pattern at the moment of breakage can be determined. In initial head impact tests on the windshield, the crack initiation occurred in some cases not under the impactor but at the outer edges of the glass or in the black print areas. In connection with crack initiation, high fragmentation rates were also observed there. However, due to the limitations of the black print in these edge areas, it was not possible to perform SCALP / photoelastic measurements. To make meaningful predictions about the fragmentation rate in the edge areas, further residual stress measurements should be conducted on windshields without black print. Additionally, further residual stress measurements should be conducted on single panes to gain insight into positions 2 and 3 (Fig. 5).

As a next step, in addition to actual tests on windshields, small samples corresponding to different fragmentation degrees will be created. These are intended to correspond to the fracture patterns that occur during the impact tests. A method is being developed to characterize and preserve this fracture pattern. Initial investigations have revealed that the fracture patterns on the upper (pos. 1) and lower panes (pos. 4) can sometimes differ significantly. Therefore, a method must first be developed to identify the cracks and their respective fracture side. In the next step, the small samples will be produced. A suitable methodology has been developed for this purpose to manufacture the samples with the desired fragmentation degree and fracture pattern. Tensile and bending tests will be conducted on these small samples at varying load rates to characterize the residual load-bearing capacity of the broken laminate. These findings will be mathematically described, then incorporated into the simulation model, and verified through further tests. This will enable small and medium-sized enterprises to predict the HIC value without full scale windshield tests.

References

- Akeyoshi, K., & Kanai, E. (1965). Mechanical Properties of Tempered Glass. In *Proceedings of the 7th international Glass Congress Vol. 14*, pp. 80-85.
- Alter, C. (2019). *Nicht-lokale Versagensformulierung zur Simulation des spannungsratenabhängigen Bruchverhaltens von Verbundsicherheitsglas und ihre Anwendung beim Kopfaufprall auf Windschutzscheiben*. Springer-Verlag.
- Angelides, S., Talbot, J. P., & Overend, M. (2021). High strain-rate effects from blast loads on laminated glass: an experimental investigation of the post-fracture bending moment capacity based on time-temperature mapping of interlayer yield stress. *Construction and Building Materials*, 273, p. 121658.
- Anglides, S. (2022). The influence of fracture pattern on the residual resistance of laminated glass at high strain-rates: an experimental investigation of the post-fracture bending moment capacity based on time-temperature mapping of interlayer yield stress. *Glass Structures & Engineering*, pp. 1-20.
- BMBF-Projekt 17N1111. (2014). *Experimentelle und numerische Untersuchungen von Windschutzscheiben unter stoßartiger Belastung zur Verbesserung des Fußgänger- und Insassenschutzes*.
- BMWi-Projekt 18295N. (2020). *Stochastisches Bruchverhalten von Glas*.
- Boilzi, L., Orlando, M., Piscitelli, L. R., & Spinelli, P. (2016). Static and dynamic response of progressively damaged ionoplast laminated glass beams. *Composite Structures* 157, pp. 337-347.
- Botz, M. (2020). *Beitrag zur versuchstechnischen und numerischen Beschreibung von Verbundglas mit PVB-Zwischenschicht im intakten und gebrochenen Zustand*. Neubiberg: Universität der Bundeswehr München.
- Glasstress Ltd. (Ver. 5.8.5). *Scattered Light Polariscopes SCALP, Instruction Manual*.
- Gross, D., Hauger, W., Schröder, J., & Wall, W. A. (2014). *Technische Mechanik 2*.
- Hooper, P. (2011). *Blast performance of silicone-bonded laminated glass*.
- Lee, H., Cho, S., Yoon, K., & Lee, J. (2012). Glass Thickness and Fragmentation Behavior in Stressed Glasses. *New J. Glas and Ceramics*.
- Mognato, E., Brocca, S., & Barbieri, A. (2017). Thermally Processed Glass : Correlation Between Surface Compression, Mechanical and Fragmentation Test. *Glass Performance Days*, pp. 8-11.
- Nielsen, J. H., & Bjarrum, M. (2017). Deformations and strain energy in fragments of tempered glass: experimental and numerical investigation. *Glass Structures & Engineering*.
- Nielsen, J., Thiele, K., Schneider, J., & Meyland, M. (2021). Compressive zone depth of thermally tempered glass. *Construction and Building Materials*.
- Pourmoghaddam, N. (2019). *On the fracture behaviour and the fracture pattern morphology of tempered soda-lime glass*. Darmstadt: Springer-Verlag.
- Pourmoghaddam, N., & Schneider, J. (2019). Experimental investigation into fragment size of tempered glass. *Glass Structures & Engineering*, 3(2), pp. 167-181.
- Pourmoghaddam, N., Kraus, M. A., Schneider, J., & Siebert, G. (2019). Relationship between strain energy and fracture pattern morphology of thermally tempered glass for the prediction of the 2D macro-scale fragmentation of glass. *Glass Structures & Engineering*, 4(2), pp. 257-275.
- Samieian, M. A., Cormie, D., Smith, D., Wholey, W., Blackman, B. R., Dear, J. P., & Hooper, P. A. (2018). Temperature effects on laminated glass at high rate. *International Journal of Impact Engineering*, 111, pp. 177-186.
- Seshadri, M., Bennison, S. J., Jagota, A., & Saigal, S. (2002). Mechanical response of cracked laminated plates. *Acta Materialia* 50(18), pp. 4477-4490.
- Wellershoff, F., & Illguth, M. (2021). Tragverhalten von gebrochenem Verbundsicherheitsglas aus Einscheibensicherheitsglas im biaxialen Spannungszustand. *ce/papers* 4(5), pp. 329-344.
- World Health Organization. (2018). *Global status report on road safety 2018*. Geneva.
- Zhao, C., Yang, J., Wang, W. E., & Azim, I. (2019). Experimental investigation into the post-breakage performance of pre-cracked laminated glass plates. *Construction and Building Materials*, 224, pp. 996-1006.